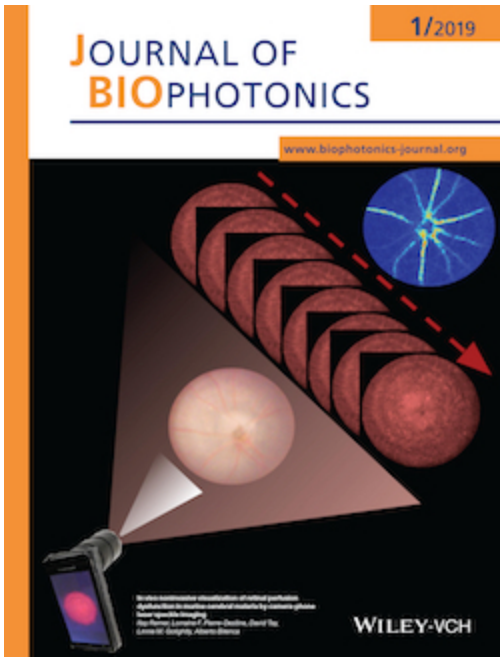

Ex vivo confocal Raman microspectroscopy of porcine dura mater supported by optical clearing

Journal:	*Journal of Biophotonics*
Manuscript ID	Draft
Wiley - Manuscript type:	Research Article
Date Submitted by the Author:	n/a
Complete List of Authors:	JAAFAR, ALI; Wigner Research Centre for Physics, Holomb, Roman; Wigner Research Centre for Physics Sdobnov, Anton ; University of Oulu Faculty of Information Technology and Electrical Engineering Ocskay, Zsombor; Semmelweis University Faculty of Medicine Jakus, Zoltán Jakus; Semmelweis University Faculty of Medicine Tuchin, Valery; Saratov State University, Chair of Optics and Biophotonics miklos, veres; Wigner Research Centre for Physics
Keywords:	Confocal Raman microspectroscopy, collagen type I, dura mater, glycerol, tissue optical clearing

Ex vivo confocal Raman microspectroscopy of porcine dura mater supported by optical clearing

Ali Jaafar *[1,2,3], Roman Holomb[1,4], Anton Y. Sdobnov[5,6], Zsombor Ocskay[7], Zoltán Jakus[7], Valery V. Tuchin[5,8,9], Miklós Veres[1].

[1] Institute for Solid State Physics and Optics, Wigner Research Center for Physics, P.O. Box 49 H-1525, Budapest, Hungary
[2] Institute of Physics, University of Szeged, Dom ter 9, H-6720 Szeged, Hungary
[3] Ministry of Higher Education and Scientific Research, 10065 Baghdad, Iraq
[4]Dept. of Information Control Systems and Technologies, Uzhhorod National University, 88015 Uzhhorod, Ukraine
[5]Science Medical Center, Saratov State University, 83 Astrakhanskaya str., 410012 Saratov, Russia
[6] Optoelectronics and Measurement Techniques Laboratory, University of Oulu, 90570 Oulu, Finland
[7]Department of Physiology, Semmelweis University School of Medicine, 1094 Budapest, Hungary
[8] Laboratory of Laser Diagnostics of Technical and Living Systems, Institute of Precision Mechanics and Control of the Russian Academy of Sciences, 24 Rabochaya str., 410028 Saratov, Russia
[9]A.N. Bach Institute of Biochemistry, Research Center of Biotechnology of the Russian Academy of Sciences, 33-2 Leninsky Prospect, 119071 Moscow, Russia
*Correspondence
Ali Jaafar, Institute for Solid State Physics and Optics, Wigner Research Center for Physics, P.O. Box 49 H-1525, Budapest, Hungary
Email: alijaafar@szfki.hu

Abstract:

In this study we report, the effect of tissue optical clearing (TOC) on porcine *dura mater* studied by confocal Raman microspectroscopy (CRM). The optical clearing of *ex vivo* tissue samples was used to increase the probing depth of CRM and to observe in-depth structure of the porcine dura mater. The Raman signal intensities were significantly increased at the depth of 250 μm for all collagen Raman bands after 30 min treatment with 99.0% glycerol as an optical clearing agent (OCA). The influence of glycerol on the *dura mater* collagen hydration was also investigated. The results indicate that the process of tissue optical clearing can be divided into two main steps. The first one is a fast process of tissue dehydration accompanied by collagen shrinkage while the second relatively slow process is related to the glycerol penetration into the

interfibrillar space of collagen combined with swelling of tissue. The potential and advantages of using the CRM and the effect of optical clearing in investigation of tissue are emphasized and discussed in detail. To the best of our knowledge, this study is the first example to introduce the TOC technique in assisting CRM of *ex vivo dura mater* in-depth probing.

Keywords: Confocal Raman microspectroscopy; collagen type I; *dura mater*; glycerol; tissue optical clearing.

Abbreviations: **CRM**: Confocal Raman Microspectroscopy; **DM**: *Dura Mater*; **OCA**: Optical Clearing Agent; **TOC**: Tissue Optical Clearing.

1 Introduction

Human DM is the supportive and protective barrier surrounding the brain. It consists of two layers: the outermost is the periosteal layer and the inner meningeal layer is illustrated in Figure 1. The first layer is attaching to the inner skull and contains branched net of blood vessels, cerebro-spinal fluid (CSF) drainage system, nerves, and large collagenous packed in lamellar bundles. The laminae are immersed in the interstitial fluid (an amorphous base substance). The second layer is dense fibrous membrane connected with the DM of the spinal cord [1]. DM is a typical fibrous tissue that contains mostly collagen fibrils which constitute more than 90% of its thickness. The average diameter of collagen fibrils assessed by electron microscopy is about 100 ± 5 nm [2]. Since the bundles of collagen fibrils are the main DM layer, measurement of its optical properties such as extremely high scattering coefficient and relatively low absorption coefficient in the visible and near-infrared wavelength regions, basically means measurement of the optical properties of the whole DM [3]. As in most fibrous structures, the indices of refraction of the main components of the DM, were found as 1.474 for collagen fibrils and 1.345

for the interstitial fluid (at the wavelength of 589 nm) [4]. It should be noted that there are no abrupt boundaries between the DM layers. They are anatomically and functionally connected to each other, constituting a single whole. Thus, due to its structure, the DM is most similar to the sclera and skin dermis. The presence of blood vessels in the DM is the major difference between the structure of the DM and sclera [1].

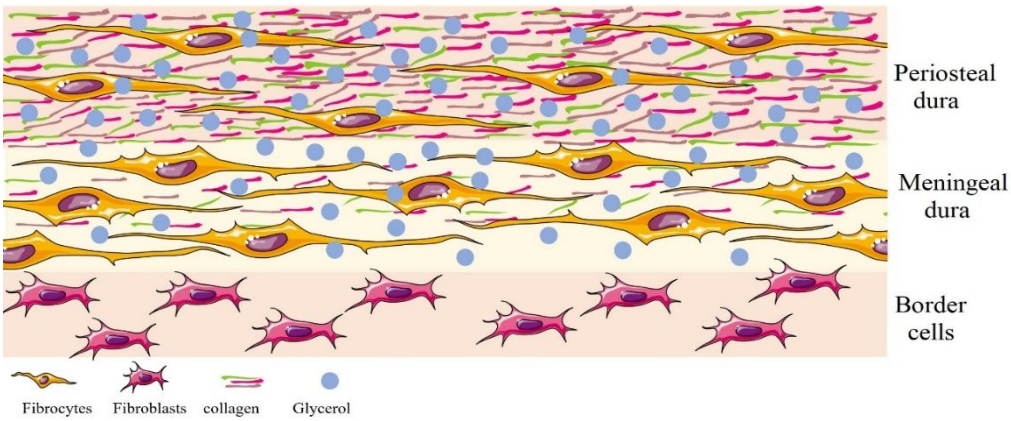

Figure 1. Schematic of immersion of *dura mater* layers into glycerol. The shapes of the cells of different types were adapted from Servier Medical Art (http://smart.servier.com/).

In the last few years, the progress in using biomedical photonic techniques for real-time monitoring of the pathophysiological change of the tissue and tissue diagnostics has been increased, because of their easy operation, low price, and minimal risks. One of the focuses of optical technology development is the design of clinical functional cerebral imaging systems to study deep inhomogeneities in tissues, aiming brain diagnostics, laser therapy and surgery [5,6]. Confocal Raman microspectroscopy (CRM) is becoming increasingly of interest in biomedical imaging techniques. CRM gives information on the molecular structure of observed biological tissue based on the detection of inelastically scattered light obtained throughout the exchange of energy between excitation light and tissue molecules. By recording the spectral distribution and intensity of the Raman scattered photons, the information on the type and concentration of

chemical bonds presents in a tissue can be obtained, since the frequency of the vibrational band observed in the Raman spectrum is determined by the bond type and the geometry of the molecular structure and, the band intensity (number of scattered photons) is proportional to the number of particular bonds in the molecules [7]. In fact, the Raman spectrum of the tissue can be taken into consideration as its distinctive molecular fingerprint containing information about the chemical conformation.

Raman spectra from tissues samples are intrinsically weak due to the low amount of inelastically scattered photons. Therefore, numbers of technologies have been developed to improve the Raman intensity. Resonance Raman scattering [8], surface-enhanced Raman scattering (SERS) [9], and tip-enhanced Raman scattering [10,11], stimulated Raman scattering (SRS) [12] are the most effective approaches.

In the case of the brain, the Raman spectrum correspond to fingerprint signatures for the chemical composition of different tissue constituents like collagen, blood, proteins, lipids, nucleic acids and tumors [13–15]. In this way, the evaluation of Raman bands permits gaining information about the biochemical properties of the observed tissue. Even insignificant changes in tissue composition lead to alterations in Raman bands position and intensity, indicating very good sensitivity and detection capabilities of this technique.

All optical imaging techniques including CRM are facing critical issues limiting the probing depth and spatial resolution due to the high level of light scattering and low absorption properties of biological tissues [16]. Considering the brain imaging, the sparing therapy and diagnostics of brain diseases, the significantly high scattering of DM in the visible and near-infrared spectra range limits the spatial resolution and depth of probing for using non-invasive optical imaging technologies [17]. One of the simplest and most effective methods to improve

the scanning depth, image quality and to increase the spectroscopic data accuracy from blood vessels network and the cerebral cortex structures is to change the optical properties of DM for some time [18–20].

In the nineties of the last century, tissue optical clearing (TOC) technique was developed and introduced with the main goal to improve the effectiveness of penetration of visible and infrared wavelengths into the deep layers of biological tissue and to enhance the probing depth for optical spectroscopic and imaging devices. The TOC allows changing the optical properties of the biological tissues, particularly, by highly reducing the light scattering properties of tissues. It was effectively implemented to improve the scanning depths of optical imaging techniques in different tissues and to enhance the contrast of the optical images, as well as to enhance the light focusing ability, and increase the spatial resolution for many non-invasive optical diagnostic methods [5,21]. The mechanisms of interaction of OCAs with tissues are not fully understood. For more detailed description of interactions between the biological tissues and OCAs can be found in the literature [4,5,22–24].

Currently, numerous optical imaging methods such as Raman spectroscopy [25], Optical Coherence Tomography [26,27], 3D-confocal microscopy [28], and polarized microscopies [29], are used in combination with different OCAs like glucose [30], dimethyl sulfoxide (DMSO), glycerol [31], uDISCO [32], *ScaleS* [33], and *Scale* [34], to increase sensitivity and improve light propagation in-depth tissues. Even though there are a vast number of research articles, very little attention has been given to investigate the effects of OCAs on different tissues. Moreover, there is no applicable information on the effect of application time and other parameters like physical penetration depth into the tissue when OCAs are combined with different optical imaging methods. These chemical agents are generally nontoxic but applying at a long exposure time and

high concentration can result in negative effects on the tissue, like extreme tissue compression, local hemostasis, and even tissue necrosis. Thus, it is significantly important to prevent or minimize the negative effect and find the most efficient agent, the harmless concentration, and the optimal exposure time, specifically for *in vivo* imaging of living tissues.

Additionally, the importance of investigating the TOC of human DM could be useful technique to examine the post-mortem of head injuries, aiding in the assessment of subdural bleeding associated with this tissue, particularly subdural hematomas [19]. Recent evidence suggests that DM endothelial cells have more angiogenic potential than brain endothelial cells that accelerated vascular regeneration in a head injury study [35]. Raman spectroscopy was used to detect the differences between dura and meningioma, related to collagen and lipid content [13],and surface-enhanced Raman scattering was also employed to detect and quantify three types of meningitis pathogens in the cerebral spinal fluid [36].

In this study, we present the results of the experimental investigation of OCA influence on probing depth using porcine DM as a human's DM model with CRM assessment. The influence of glycerol on Raman spectra and intensities of principal collagen peaks has been investigated using CRM. To the best of our knowledge there is no information about using CRM for investigation of DM combined with TOC technique in-depth probing.

2 MATERIALS AND METHODS

2.1 Reagents and sample preparation

The glycerol is known as the most frequently used and effective OCA for application to tissue due to its biocompatibility, pharmacokinetics, and high index of refraction. Therefore, glycerol of 99.0% purity (purchased from Sigma-Aldrich Ltd.) was used in this study. To study the TOC, fresh porcine DM was chosen. *Ex vivo* porcine DM may serve as the model of *in vivo*

human DM due to its a gross anatomical structure, housing, feasibility and ethical considerations [37–39].

The DM samples were taken from 12 pigs provided by the local accredited abattoir (Albertirsa, Hungary) and kept cold on ice in phosphate-buffered saline. Before the measurement, DM was wiped with a paper towel. The tissue samples of 22 mm^2 size were prepared for investigation of TOC effect, a leather punch was used to cut the samples. Finally, the tissue samples were placed in Petri dishes filled with 5mL of 99.0% glycerol for 5,10,15 and 30 minutes. DM without the OCA treatment (*i.e.,* untreated tissue) was used as a control sample. The thickness of each sample was measured using a digital micrometer before and after TOC. All CRM measurements were performed by placing the tissue samples on silicon substrates for easier handling and examination through the outer endosteal layer.

2.1.1 Confocal Raman microspectroscopy

Raman spectra were obtained in the backscattered geometry and confocal mode by using an inVia^{TM} Raman microscope (Renishaw, UK). To obtain the depth profile (Z) of porcine DM, samples were placed on a computer-controlled three-axis motorized stage which allows the vertical movements of the sample with micrometer resolution see Figure 2; a 633 nm laser source was used for the measurements with 1200 g/mm gratings. The measurements were performed with spatial resolution of 0.77 µm and spot size of 1.5 µm.

For the spontaneous Raman scattering, the Raman intensity is approximately inversely proportional to the fourth power of the excitation laser wavelength. Therefore, a shorter wavelength may be suitable to improve the sensitivity. Additionally, 633 nm laser was chosen because the sensitivity (quantum efficiency) of the CCD detectors response is highly decreased in the near-infrared range leading to weaker Raman scattering efficiency. The CCD efficiency is

rapidly reducing for high wavenumbers which are important for the estimation of tissue water content and lipid characterization [40,41]. The CCD detector at 633 nm is allowing the maximum sensitivity to cover both fingerprint and high wavenumbers region. In this way, the admission of TOC method with CRM using 633 nm will allow achieving both high probing depth and spectral resolution for tissue measurements [42]. The laser beam was focused on the sample by a 50x objective, and the Raman spectra were collected also with it. To prevent tissue damage, the delivered laser power on the DM surface was kept at 8.3 mW. The Raman spectra were collected with 5 seconds of laser exposure time at three different spots on each sample. Before measurements, extra OCAs were removed from the surface of the sample using a paper towel. All spectra were recorded and analyzed in the molecular fingerprint spectral region from 400 to 1800 cm^{-1}. Before the Raman measurements, the system was spectrally calibrated using the 520 cm^{-1} Raman band of a silicon wafer. All recorded spectra from each sample were averaged, then processed and analyzed using the Spectragryph software. The spectra processing includes the baseline correction using a polynomial function and curve smoothing using the Savitzky–Golay filter (3rd-order polynomial and 9 points interval) [43].

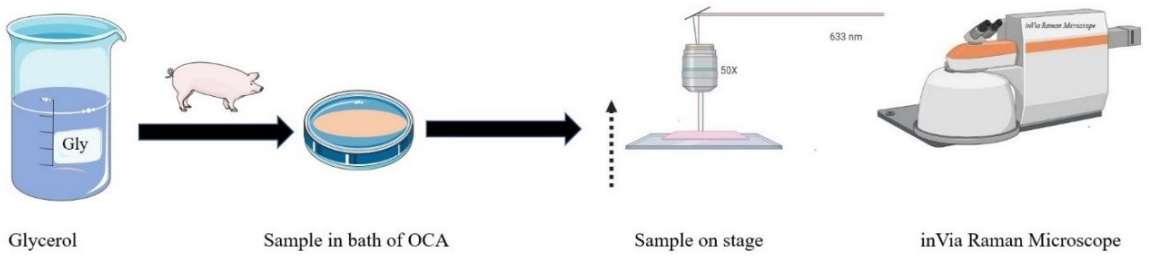

Figure 2. Schematics of the experimental setup. The shapes were adapted from Servier Medical Art (http://smart.servier.com/).

3 RESULTS AND DISCUSSION

Figure 3 illustrates the examples of series of Raman spectra obtained from the untreated DM at different depths ranging (from 0 to 250 μm) with 25 μm step size. The principal Raman peaks of the DM corresponding to collagen can be identified by the presence of four Raman peaks at 938 cm^{-1} (C–C stretching mode of collagen), 1246 cm^{-1} (amide III), 1268 cm^{-1} (amide III), and 1666 cm^{-1} (amide I).

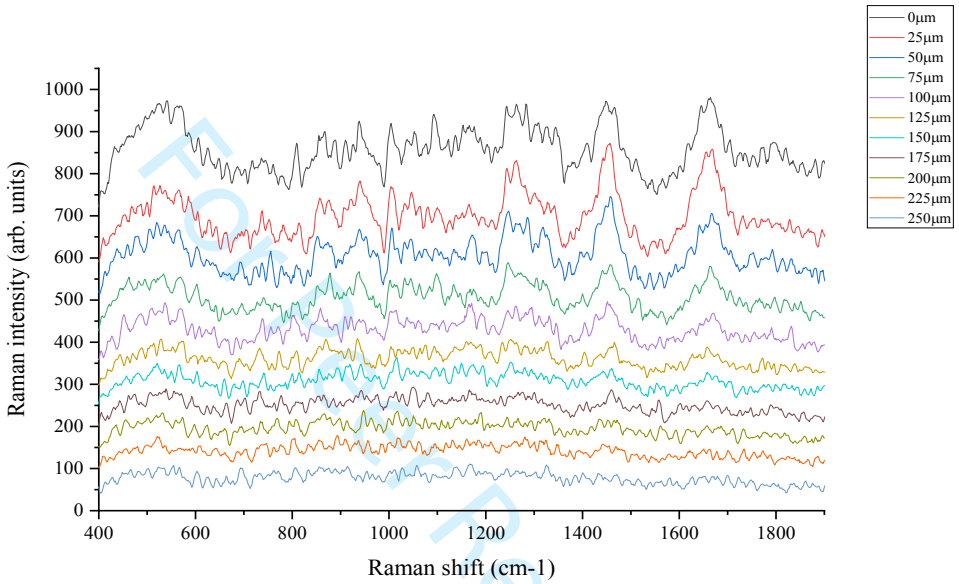

Figure 3. Evolution of the Raman spectra of untreated porcine *dura mater* in the fingerprint region measured at different depths from 0 to 250 μm. The spectra were offset along the ordinate for clarity.

The DM tissue is highly scattering in the visible and near-infrared regions due to the mismatching between refractive indices of the collagen fibers and interstitial fluid. The tissue scattering significantly attenuates the power of probing light source and causes the focused beam to spread which leading to reduction of signal detected by the CRM. As a result, the intensities of Raman bands get weaker with increasing depth into the DM. It is clearly seen from Figure 3 that the Raman intensity drastically diminished with the increased depth of investigation due to the limited focus light penetration into porcine DM. As can be seen, the Raman bands cannot be

efficiently resolved at the depth of 75 to 250 μm, which can be ascribed to fewer number of probing and detected photons caused by high scattering and absorption properties of the collagen tissue. Because of the cellular and subcellular structures with varying refraction indices, fewer photons can travel to deepest DM regions and at the same time, less Raman-backscattered photons can be detected from there, as well.

The glycerol treatment of DM improves the quality of the Raman bands in the Raman spectra of tissue measured at deeper regions, thus allowing the deeper layer to be investigated and analyzed in detail. Figure 4 illustrates the unique vibrational bands in the Raman spectrum of glycerol excited using 633 nm laser. The main Raman peaks of glycerol appear at 484 and 1056 cm^{-1}. In previous studies, it has been demonstrated that the application of glycerol on tissues could efficiently enhance the Raman to fluorescence ratio and signal contrast [44,45]. The principal peaks for glycerol can be resolved at Raman spectra at all depths after the treatment, indicating that during the experiment the OCA is penetrated to all observed depths during the experiment of the tissue.

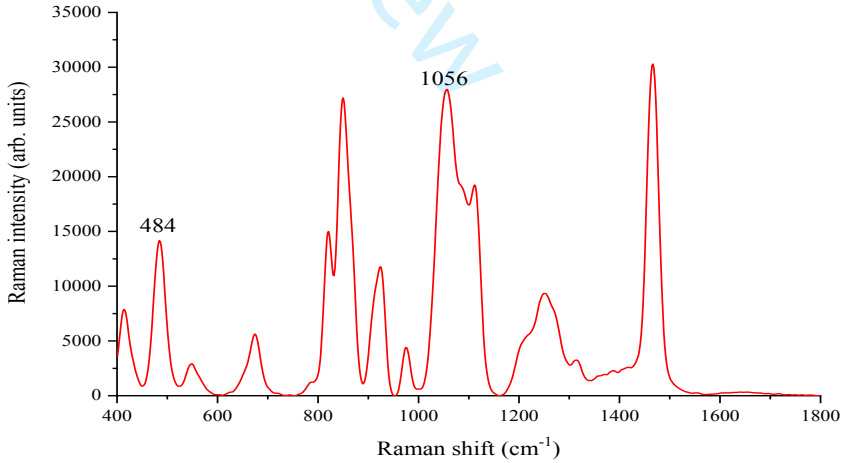

Figure 4. Raman spectrum of 99.0 % glycerol.

To study the optical clearing process of DM using 99.0% glycerol, the Raman bands of untreated and treated porcine DM were obtained at different depths. The depth dependent Raman spectra of porcine DM after 5, 10, 15 and 30 min glycerol treatment are shown in Figure 5A, 5B, 5C and 5D, respectively. In order to allow direct comparison between TOC results at different depths, the DM spectra were firstly baseline corrected and normalized on the amide I band (from 1590 to 1750 cm^{-1}) [40,46,47].

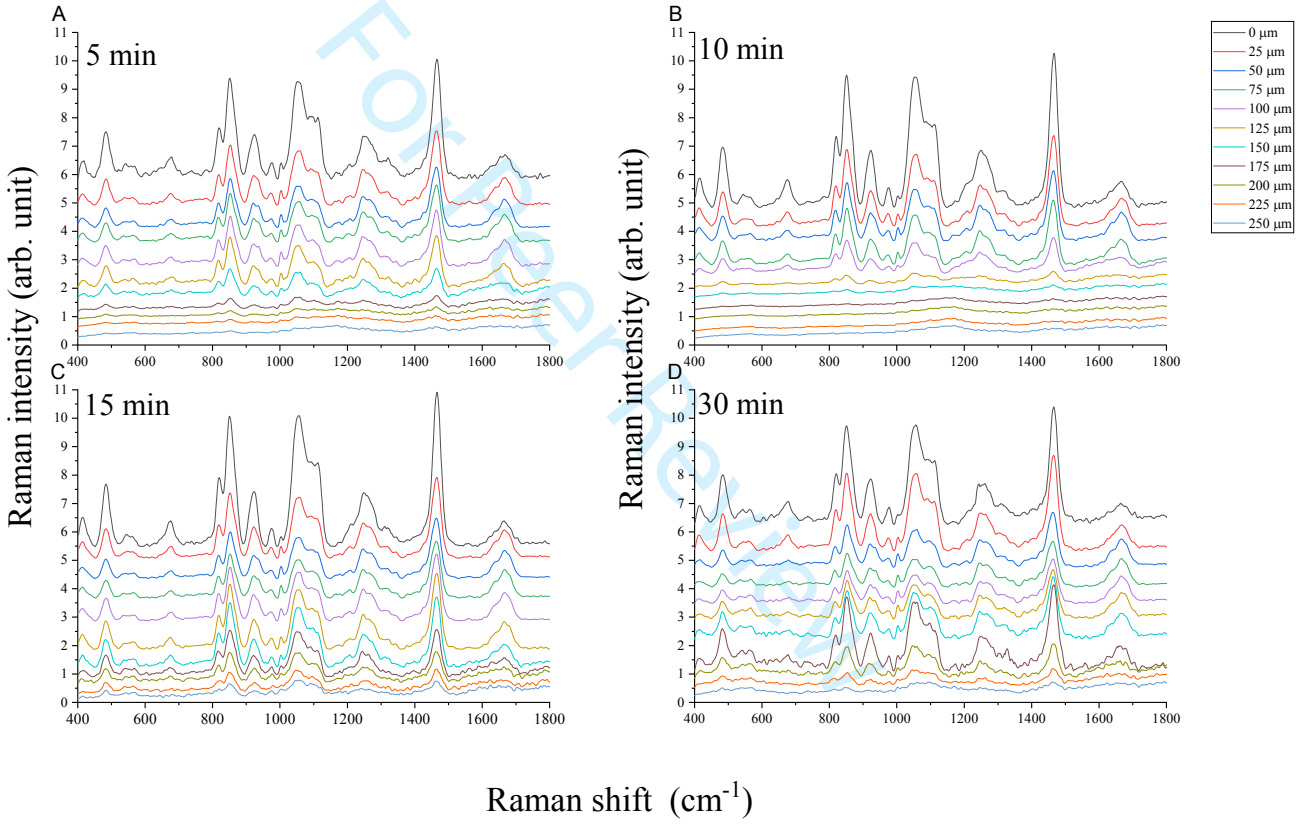

Figure 5. Evolution of averaged Raman spectra of A) 5 min, B)10 min, C)15 min, and D)30 min treated porcine *dura mater* with 99.0% glycerol from depths of 0 to 250 μm in the fingerprint region (400 to 1800 cm^{-1}). All spectra were excited with 633 nm laser and recorded using the same conditions.

As can be seen from Figure 5 A-D the vibrational bands observed in the Raman spectra of the treated DM are much higher in intensities in comparison with the corresponding band intensities of the untreated sample Figure 3. Such behavior is especially seen in the Raman spectra measured from the deeper layers of treated DM. Therefore, the TOC effect can directly be detected by CRM. Also, it is clearly seen from Figure 5 A-D that the glycerol effect depends on treatment time. To perform quantitative investigation of time-dependence of TOC effect at different depths, it is necessary to compare the spectra obtained at different depths and for different treatment times. To compare the improvement due to TOC, the intensities of the main bands of collagen observed in the depth-dependent (0-250 μm) Raman spectra of porcine DM treated with 99.0% glycerol for 0, 10, 15 and 30 min were examined. The results summarized in Figure 6 show the kinetic curves that reveal the effect of treatment time on the intensity of Raman bands of collagen located at 938, 1246, 1268 and 1666 cm^{-1}.

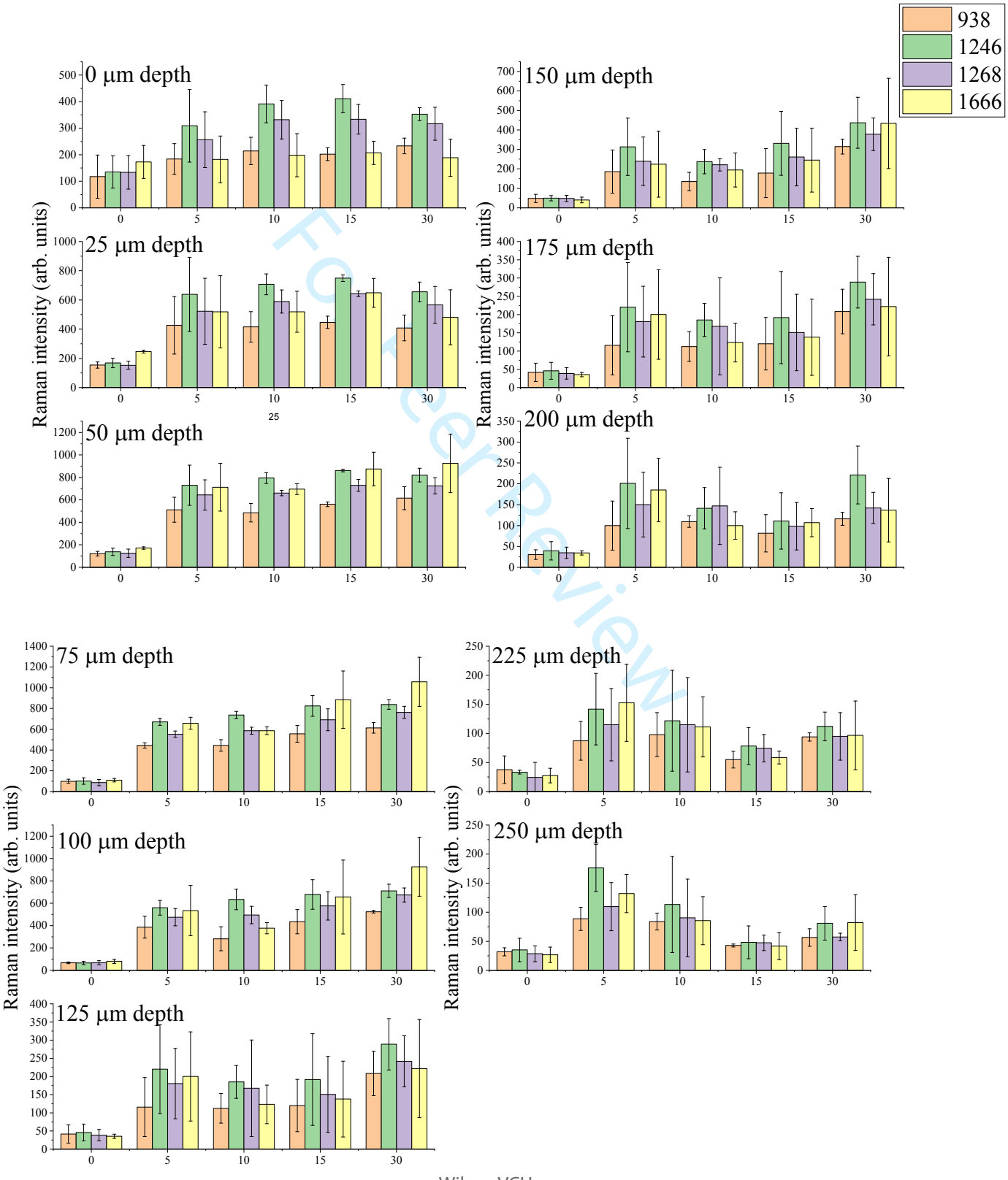

Figure 6. The time-dependency of dura mater-based Raman bands at 938 cm^{-1} ,1246 cm^{-1},1268 cm^{-1} and 1666 cm^{-1} after application of 99.0% glycerol at different depths from 0 to 250 μm.

It can be seen that the Raman band intensities are increasing after TOC treatment due to refractive index matching and dehydration process caused by glycerol [48], thus, more compact organization of collagen fibers and less light scattering. Also, the application of OCA results in increased penetration depth of focused light through the DM tissue [49,50], leading to improvement of the Raman signal from in-depth tissues layers. The scattering of laser light in the upper layers of turbid tissue is strongly anisotropic and balances elastic scattering and linear absorption [51].

For the depths ranging from 0 to 50 μm the intensities of Raman bands of DM are monotonically increasing after TOC followed by saturation of the dependence occurring at 15 min treatment after which the intensities start to reduce. In the depth range of 75 to 125 μm the intensities of Raman bands corresponding to porcine DM show a monotonic increase with

respect to treatment time and achieved maximum at 30 min. This was most likely due to tissue dehydration caused by the osmotic properties of glycerol [40,45], as shown in Figure 7.

For the depths ranging from 150 to 200 μm the intensities of Raman bands of DM are decreasing after TOC, where rehydration took place in 10 min treatment, due to accumulation of water coming from deeper tissue layers (where there is no glycerol). This behavior is in good agreement with our results, as shown in Figure 9.

The 938 and 922 cm^{-1} Raman bands characteristics of stretching vibration of skeletal

C–C bonds and the stretching vibration of the C–C bond found in collagen chains, respectively.

The ratio of these band intensities tends to increase with increasing collagen hydration. Therefore, this ratio (I_{938}/I_{922}) as a function of OCA treatment time is defined as a potential spectroscopic marker of collagen hydration [52,53]. Figure 7 shows the collagen hydration rate for DM calculated at different depths ranging from 0 to 250 µm. As it can be seen from Figure 7 this ratio is dramatically decreased for all depths during the first 10 min of OCA application. The observed effect can related to the strong dehydration process caused by glycerol (replacement of DM water molecules by glycerol). In addition, after 10 min of sample treatment the I_{938}/I_{922} ratio is slightly increased for 75 to 125 µm depths. It can be related with the rehydration of collagen in DM, due to the replacement of DM water in the upper layers with water accumulate from deeper tissue layers from depth 150 to 200 µm [54]. It can be seen the ratio is decreasing after 5 min of treatment and increasing after 10 min of treatment then decreasing after 15 and 30 min of treatment. For a longer treatment time, the glycerol diffusion into the sample provides its overall rehydration expressed as

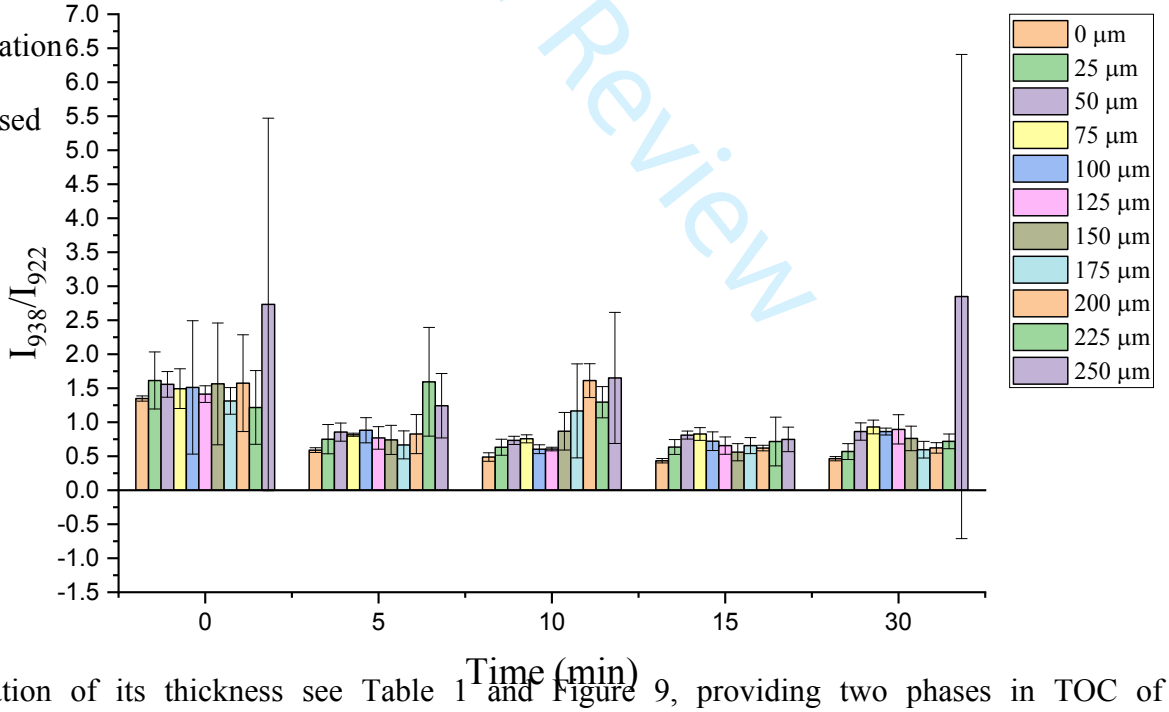

restoration of its thickness see Table 1 and Figure 9, providing two phases in TOC of collagenous tissue, fast shrinkage first and then swelling, because after penetration into tissue, the glycerol molecule can accumulate approx. six molecules of water in tissue [55,56].

Figure 7. The intensity ratio of 938 and 922 cm^{-1} Raman modes(I_{938}/I_{922}) as a function of treatment time for DM type I collagen from 0 to 250 μm depths range.

The Raman bands in 1600 to 1750 cm^{-1} spectral region typically consist of four major bands located at 1616, 1645, 1666 and 1681cm^{-1} (ν(C═C) in phenylalanine and tyrosine; amide I related to both α-helix and β-sheet; amide I α-helical conformation; and amide I disordered structure, non-hydrogen bonds, and C═O stretching, respectively). The Raman band at 1666 cm^{-1} was considered as a sensor mode of structural modifications of the amide group [57]. Therefore, spectral shift toward lower wavenumbers of the 1645 and 1666 cm^{-1} bands could be represented as an indication of the appearance of heavier structures in α-helix and β-sheet of collagen [58]. To estimate the spectral shift, Gaussian-Lorentzian deconvolution is applied after subtracting the baseline in the 1590–1720 cm^{-1} range in order to obtain repeatable and biochemically reasonable results. The full widths at half maximum FWHM of the 4 Gaussian-Lorentzian bands were permitted to change within a limited range of 20 cm^{-1} see Figure 8. Principal component analysis (PCA) was applied to reduce the low variability components of the

Raman spectra in the fingerprint range that were defined as noise. The first four principal components (PCs) are chosen to reconstruct the Raman spectra [59,60].

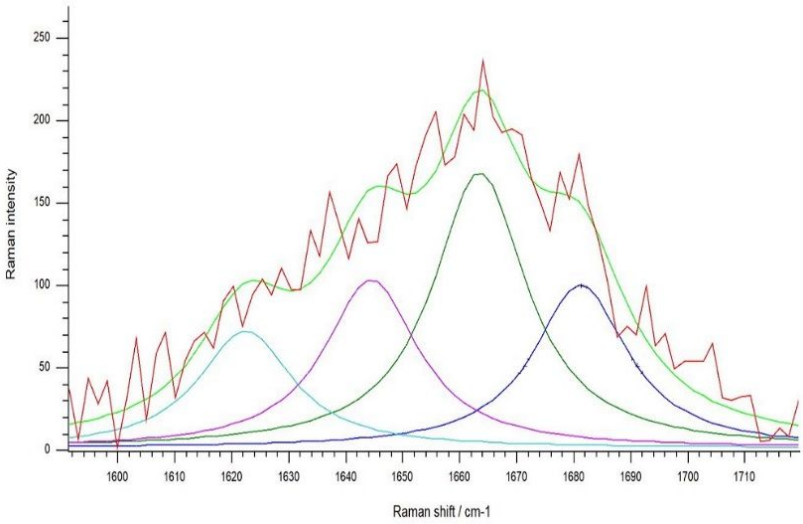

Figure 8. 4 Gaussian-Lorentzian deconvolutions of the Amide I band of untreated dura mater (at depth 25 μm) centered at 1616 ± 5 cm^{-1}, 1645± 5 cm^{-1}, 1666 ± 5 cm^{-1} and 1681± 5 cm^{-1}.

The spectral upshift of the 1645 and 1666 cm^{-1} bands as function of depth at different treatment times is shown in Figure 9. As it can clearly be seen, the behavior of upshift in wavenumber has the same trend: increasing after the treatment. The spectral shift of band at 1666 cm^{-1} illustrates the alterations in molecular geometry of amide I, due to the degradation of collagen triple helix chains and their dissociation into simple or double strings [58].

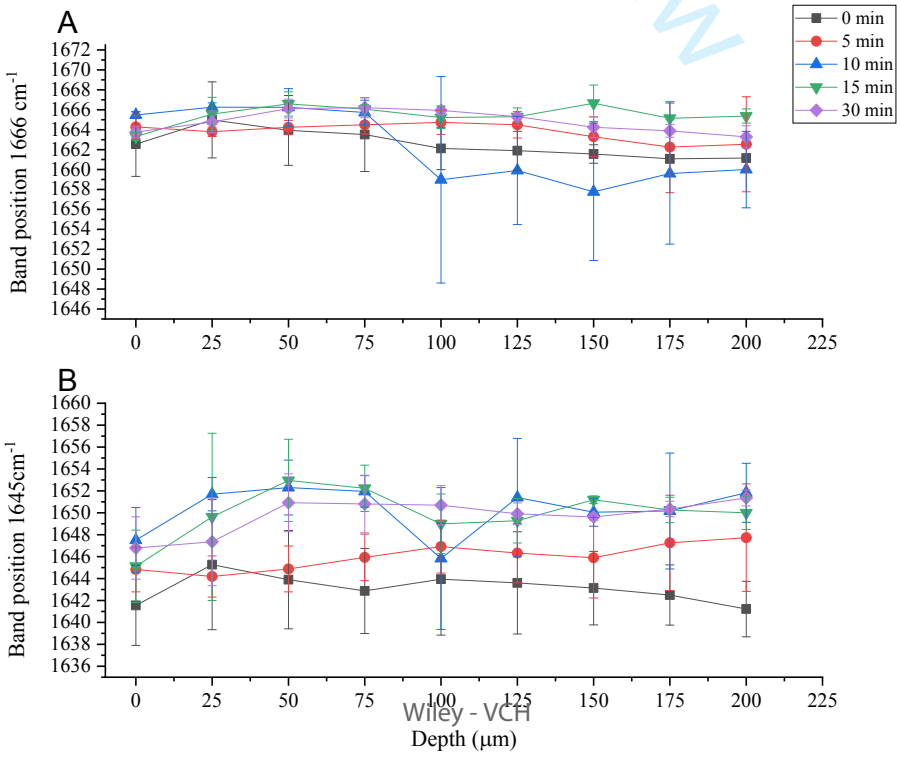

Figure 9. Evolution of the position of A) 1666 cm^{-1} and, B) 1645 cm^{-1} bands as function of depth at different treatment times.

One of the important points in assessing the TOC effect is the need to precisely measure the thickness of tissue samples during OC. Here, the measurement of thickness of DM was performed only before and after the application of the glycerol as an OCA. However, the measurements introduced in this paper showed the limits of possible changes in the geometric parameters of the DM under the action of glycerol. This makes it possible to utilize non-invasive optical imaging techniques such as OCT or confocal microscopy to monitor the thickness of DM, the change in the index of refraction during the treatment of DM with OCA should also be taken into account [5]. The measured values, showing the limits of possible changes in the geometric parameters of DM after the treatment with OCA are summarized in Table 1. The results show that the differences in thickness shrinkage/swelling of DM can be correlated with variability from animal to animal. Despite the variability of data presented in Table 1, the averaged values calculated for all samples treated for 5 to 20 min show the shrinkage of DM tissue from 0.515 mm to about 0.396 mm in the first 5 min of treatment, caused by tissue dehydration. Then due to rehydration process, the thickness reverts to its original value for 30 min treatment, up to 30 min shrinkage is not seen. For the longest time of treatment of DM tissue swelling is expected as seen in Figure 10. Such behaviour is well fit to an expression of occludin proteins in tissues as a reaction to osmotic stress due to depolymerization of microfilaments or microtubules [61,62]. Moreover, glycerol has been applied as an osmotic adjuvant to reduce intracranial hypertension

Sample	S1	S2	Ave	STD
before	0.540±0.089	0.490±0.088	0.515	0.035
after 5min	0.460±0.089	0.332±0.090	0.396	0.091
Sample	**S3**	**S4**	**Ave**	**STD**
before	0.376±0.094	0.546±0.099	0.461	0.120
after 10 min	0.378±0.071	0.384±0.044	0.381	0.004
Sample	**S5**	**S6**	**Ave**	**STD**
before	0.664±0.049	0.610±0.057	0.637	0.038
after 15min	0.500±0.064	0.356±0.034	0.428	0.101
Sample	**S7**	**S8**	**Ave**	**STD**
before	0.540±0.082	0.554±0.042	0.547	0.009
after 20 min	0.382±0.068	0.332±0.034	0.357	0.035
Sample	**S9**	**S10**	**Ave**	**STD**
before	0.360±0.127	0.480±0.065	0.420	0.084
after 25 min	0.426±0.090	0.440±0.089	0.433	0.009
Sample	**S11**	**S12**	**Ave**	**STD**
Before	0.442±0.038	0.520±0.058	0.481	0.055
after 30 min	0.510±0.103	0.430±0.059	0.470	0.056

[63]. It is important to note that in order to prevent the strong swelling of collagenous tissue under the action of OCA in ex vivo experiments, the treatment time must be less than one hour [64].

Table1. The thickness of DM samples (in mm) before and after 99.0% glycerol treatment for 5, 10, 15, 20, 25 and 30 min. Two samples were measured for each treatment time and the thickness was measured in 5 different points on each of them. The measurements were performed on DM samples sandwiched between two glass plates by using a micrometer

.

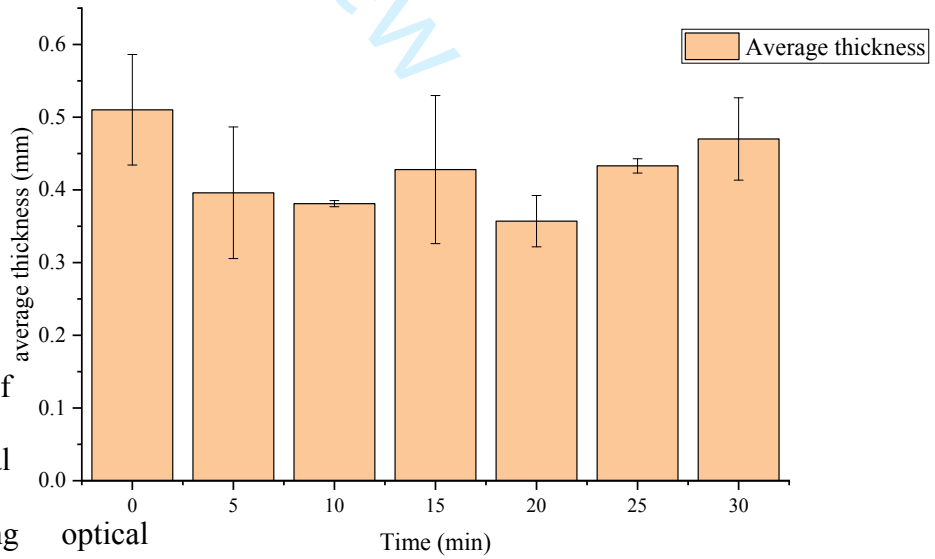

Figure 10. *Dura mater* average thickness (in mm) as function of treatment time.

A previous study of glycerol effect on the thermal properties of collagen using optical displacement-enhanced heterodyne polarimeter shows improvement of thermal denaturation of

collagen [65]. Using glycerol as an OCA in combination with magnetite nanoparticles studies of laser heating of costal cartilage shown to be effective [66]. Moreover, glycerol interaction with collagen is important in the context of the suitability of the collagenous tissue as a dural graft in the repair of spinal dura mater defects[67,68].

The inherently weak Raman scattering efficiency and the high scattering of the turbid tissue limits its utilization to superficial locations and to extend the applications of a Raman to deep tissues, the tissue optical clearing and metallic nanoparticles combination and utilization of surface-enhanced Raman scattering will be promising approach for the extension of the clinical applications of confocal Raman microspectroscopy from superficial to deeper tissues to detect metastatic sentinel lymph nodes[69,70].

4 CONCLUSIONS

Ex vivo investigation of optical clearing of porcine dura mater was performed by using confocal Raman microspectroscopy, including the detailed spectroscopic depth profiling of the tissue. The results show that by using glycerol as an OCA for 30 min of treatment time the information depth of porcine DM can significantly be extended. This improvement is due to the reduction of light scattering in the tissue increasing the propagation depth of optical radiation into DM by keeping the focusing of the laser beam. As TOC is a dynamic technique, CRM was also successfully used to study the TOC processes related to collagen fibers. The results indicate that the process of tissue optical clearing can be divided into two main steps. The first one is a fast process of tissue dehydration accompanied by collagen shrinkage, while the second relatively slow process is related to the glycerol penetration into the interfibrillar space of collagen combined with swelling of tissue.

The enhancement of capability of laser light penetration into a DM tissue and, consequently, incensement of the probing depth by controlling the optical parameter is a useful technique and can be applied in laser therapeutic and optical diagnostic and imaging techniques of brain tissues. In addition, these results could be useful for forensic purposes and Burr holes application. The further work is necessary to define the optimal laser wavelength to study *Dura mater* disease related to collagen with different OCAs and nanoparticles.

Acknowledgments

This work was done under a scholarship of the Stipendium Hungaricum Scholarship Programme. This work was supported by the VEKOP-2.3.2-16-2016-00011 and VEKOP-2.3.2-16-2016-00002 grants, which are co-financed by the European Union and European Social Fund. VVT was supported the grant of the Government of the Russian Federation 075-15-2019-1885. In addition, we would like to appreciate the support of Dr. Riana Gaifulina.

Conflicts of Interest

The authors declare that there are no conflicts of interest relevant to this article.

DATA AVAILABILITY STATEMENT

Research data are not shared

REFERENCES

[1] V.I. Ziablov, I.N. Shapovalov, K.D. Toskin, V. V. Tkach, V. V. Zhebrovskiĭ, Structure and physicomechanical properties of the human dura mater from the age aspect, Arkh. Anat. Gistol. Embriol. 82 (1982) 29–36. https://pubmed.ncbi.nlm.nih.gov/7092586/ (accessed July 1, 2021).

[2] A.N. Bashkatov, E.A. Genina, Y.P. Sinichkin, V.I. Kochubey, N.A. Lakodina, V. V. Tuchin, Glucose and Mannitol Diffusion in Human Dura Mater, Biophys. J. 85 (2003) 3310–3318. https://doi.org/10.1016/S0006-3495(03)74750-X.

[3] A.N. Bashkatov, E.A. Genina, V. V. Tuchin, Tissue optical properties, in: Handb. Biomed. Opt., CRC Press, 2016: pp. 67–101. https://doi.org/10.1201/b10951-9.

[4] V. V. Tuchin, Optical clearing of tissues and blood, PM 154, SPIE Press. Bellingham, WA,. (2005) 1–255. https://doi.org/10.1117/3.637760.

[5] V. V Tuchin, Tissue Optics : Light Scattering Methods and Instruments for Medical Diagnostics, 3rd ed., PM 254, SPIE Press, Bellingham, WA, 2015– 988 p. https:/pie.org/Publications/Book/2175698, 2015.

[6] V.V. Tuchin, Handbook of Optical Biomedical Diagnostics. Light-Tissue Interaction, Vol.1, 2nd ed., SPIE Press PM262, Bellingham, WA, USA, 2016 – 864 p., (2016). https://spie.org/Publications/Book/2219613?SSO=1 (accessed August 10, 2021).

[7] P.J. Aarnoutse, J.A. Westerhuis, Quantitative Raman reaction monitoring using the solvent as internal standard, Anal. Chem. 77 (2005) 1228–1236. https://doi.org/10.1021/ac0401523.

[8] Y. Zhou, C.-H. Liu, Y. Sun, Y. Pu, S. Boydston-White, Y. Liu, R.R. Alfano, Human brain cancer studied by resonance Raman spectroscopy, J. Biomed. Opt. 17 (2012) 116021. https://doi.org/10.1117/1.jbo.17.11.116021.

[9] L.E. Jamieson, S.M. Asiala, K. Gracie, K. Faulds, D. Graham, Bioanalytical measurements enabled by Surface-Enhanced Raman Scattering (SERS) probes, Annu. Rev. Anal. Chem. 10 (2017) 415–437. https://doi.org/10.1146/annurev-anchem-071015-041557.

[10] R. Zhang, X. Zhang, H. Wang, Y. Zhang, S. Jiang, C. Hu, Y. Zhang, Y. Luo, Z. Dong, Distinguishing Individual DNA Bases in a Network by Non-Resonant Tip-Enhanced Raman Scattering, Angew. Chemie. 129 (2017) 5653–5656. https://doi.org/10.1002/ange.201702263.

[11] C. Gullekson, L. Lucas, K. Hewitt, L. Kreplak, Surface-sensitive Raman spectroscopy of collagen I fibrils, Biophys. J. 100 (2011) 1837–1845. https://doi.org/10.1016/j.bpj.2011.02.026.

[12] K.S. Shin, A.T. Francis, A.H. Hill, M. Laohajaratsang, P.J. Cimino, C.S. Latimer, L.F. Gonzalez-Cuyar, L.N. Sekhar, G. Juric-Sekhar, D. Fu, Intraoperative assessment of skull base tumors using stimulated Raman scattering microscopy, Sci. Rep. 9 (2019) 1–12. https://doi.org/10.1038/s41598-019-56932-8.

[13] S. Koljenović, T.B. Schut, A. Vincent, J.M. Kros, G.J. Puppels, Detection of meningioma in dura mater by Raman spectroscopy, Anal. Chem. 77 (2005) 7958–7965. https://doi.org/10.1021/ac0512599.

[14] A. Mizuno, T. Hayashi, K. Tashibu, S. Maraishi, K. Kawauchi, Y. Ozaki, Near-infrared FT-Raman spectra of the rat brain tissues, Neurosci. Lett. 141 (1992) 47–52. https://doi.org/10.1016/0304-3940(92)90331-Z.

[15] A. Mizuno, H. Kitajima, K. Kawauchi, S. Muraishi, Y. Ozaki, Near-infrared Fourier

transform Raman spectroscopic study of human brain tissues and tumours, J. Raman Spectrosc. 25 (1994) 25–29. https://doi.org/10.1002/jrs.1250250105.

[16] Y. Zhang, H. Liu, J. Tang, Z. Li, X. Zhou, R. Zhang, L. Chen, Y. Mao, C. Li, Noninvasively Imaging Subcutaneous Tumor Xenograft by a Handheld Raman Detector, with the Assistance of an Optical Clearing Agent, ACS Appl. Mater. Interfaces. 9 (2017) 17769–17776. https://doi.org/10.1021/acsami.7b04205.

[17] A.N. Bashkatov, E.A. Genina, V.I. Kochubey, Y.P. Sinichkin, A.A. Korobov, N.A. Lakodina, V. V. Tuchin, in vitro study of control of human dura mater optical properties by acting of osmotical liquids, Control. Tissue Opt. Prop. Appl. Clin. Study. 4162 (2000) 182–188. https://doi.org/10.1117/12.405939.

[18] E.A. Genina, A.N. Bashkatov, V.I. Kochubey, V. V. Tuchin, Optical clearing of human dura mater, Opt. Spectrosc. 98 (2005) 470–476. https://doi.org/10.1134/1.1890530.

[19] E.C. Cheshire, R.D.G. Malcomson, S. Joseph, M.J.B. Biggs, D. Adlam, G.N. Rutty, Optical clearing of the dura mater using glycerol: a reversible process to aid the post-mortem investigation of infant head injury, Forensic Sci. Med. Pathol. 11 (2015) 395–404. https://doi.org/10.1007/s12024-015-9691-7.

[20] E. Genina, A. Bashkatov, V. Tuchin, Optical clearing of human dura mater by glucose solutions, J. Biomed. Photonics Eng. 3 (2017) 010309. https://doi.org/10.18287/jbpe17.03.010309.

[21] V. V. Tuchin, I.L. Maksimova, D.A. Zimnyakov, I.L. Kon, A.K. Mavlutov, A.A. Mishin, Light propagation in tissues with controlled optical properties, J. Biomed. Opt. 2 (1997) 401–417. https://doi.org/10.1117/12.281502.

[22] A.Y. Sdobnov, M.E. Darvin, E.A. Genina, A.N. Bashkatov, J. Lademann, V. V. Tuchin, Recent progress in tissue optical clearing for spectroscopic application, Spectrochim. Acta - Part A Mol. Biomol. Spectrosc. 197 (2018) 216–229. https://doi.org/10.1016/j.saa.2018.01.085.

[23] L.M.C. Oliveira, V.V. Tuchin, The Optical Clearing Method - A New Tool for Clinical Practice and Biomedical Engineering, Basel Springer Nat. Switz. AG. (2019) ,p177. https://www.springer.com/gp/book/9783030330545 (accessed March 12, 2021).

[24] V. V. Tuchin, I.L. Maksimova, D.A. Zimnyakov, I.L. Kon, A.K. Mavlutov, A.A. Mishin, Light propagation in tissues with controlled optical properties, Proc. SPIE - Int. Soc. Opt. Eng. 2925 (1996) 118–142. https://doi.org/10.1117/12.281502.

[25] M. V. Schulmerich, J.H. Cole, K.A. Dooley, M.D. Morris, J.M. Kreider, S.A. Goldstein, Optical clearing in transcutaneous Raman spectroscopy of murine cortical bone tissue, J. Biomed. Opt. 13 (2008) 021108. https://doi.org/10.1117/1.2892687.

[26] O. Zhernovaya, V. V. Tuchin, M.J. Leahy, Enhancement of OCT imaging by blood optical clearing in vessels-A feasibility study, Photonics Lasers Med. 5 (2016) 151–159. https://doi.org/10.1515/plm-2016-0004.

[27] Y. Liang, W. Yuan, J. Mavadia-Shukla, X. Li, Optical clearing for luminal organ imaging with ultrahigh-resolution optical coherence tomography, J. Biomed. Opt. 21 (2016) 081211. https://doi.org/10.1117/1.jbo.21.8.081211.

[28] Y.Y. Fu, S.C. Tang, Optical clearing facilitates integrated 3D visualization of mouse ileal microstructure and vascular network with high definition, Microvasc. Res. 80 (2010) 512–521. https://doi.org/10.1016/j.mvr.2010.06.003.

[29] O. Nadiarnykh, P.J. Campagnola, Retention of polarization signatures in SHG microscopy of scattering tissues through optical clearing, Opt. Express. 17 (2009) 5794.

https://doi.org/10.1364/oe.17.005794.
[30] K. V Larin, V. V Tuchin, Functional imaging and assessment of the glucose diffusion rate in epithelial tissues in optical coherence tomography, Quantum Electron. 38 (2008) 551–556. https://doi.org/10.1070/qe2008v038n06abeh013850.
[31] X. Zhu, L. Huang, Y. Zheng, Y. Song, Q. Xu, J. Wang, K. Si, S. Duan, W. Gong, Ultrafast optical clearing method for three-dimensional imaging with cellular resolution, Proc. Natl. Acad. Sci. U. S. A. 166 (2019) 11480–11489. https://doi.org/10.1073/pnas.1819583116.
[32] C. Pan, R. Cai, F.P. Quacquarelli, A. Ghasemigharagoz, A. Lourbopoulos, P. Matryba, N. Plesnila, M. Dichgans, F. Hellal, A. Ertürk, Shrinkage-mediated imaging of entire organs and organisms using uDISCO, Nat. Methods. 13 (2016) 859–867. https://doi.org/10.1038/nmeth.3964.
[33] H. Hama, H. Hioki, K. Namiki, T. Hoshida, H. Kurokawa, F. Ishidate, T. Kaneko, T. Akagi, T. Saito, T. Saido, A. Miyawaki, ScaleS: An optical clearing palette for biological imaging, Nat. Neurosci. 18 (2015) 1518–1529. https://doi.org/10.1038/nn.4107.
[34] H. Hama, H. Kurokawa, H. Kawano, R. Ando, T. Shimogori, H. Noda, K. Fukami, A. Sakaue-Sawano, A. Miyawaki, Scale: A chemical approach for fluorescence imaging and reconstruction of transparent mouse brain, Nat. Neurosci. 14 (2011) 1481–1488. https://doi.org/10.1038/nn.2928.
[35] B.I. Koh, H.J. Lee, P.A. Kwak, M.J. Yang, J.H. Kim, H.S. Kim, G.Y. Koh, I. Kim, VEGFR2 signaling drives meningeal vascular regeneration upon head injury, Nat. Commun. 11 (2020) 1–17. https://doi.org/10.1038/s41467-020-17545-2.
[36] K. Gracie, E. Correa, S. Mabbott, J.A. Dougan, D. Graham, R. Goodacre, K. Faulds, Simultaneous detection and quantification of three bacterial meningitis pathogens by SERS, Chem. Sci. 5 (2014) 1030–1040. https://doi.org/10.1039/c3sc52875h.
[37] F.H. Michael Frink, Hagen Andruszkow, Christian Zeckey, Christian Krettek, Experimental trauma models: An update, J. Biomed. Biotechnol. (2011). https://doi.org/10.1155/2011/797383.
[38] R.B. Emilia Mazgajczyk , Krzysztof Ścigała , Marcin Czyż , Włodzimierz Jarmundowicz, Mechanical properties of cervical dura mater, Acta Bioeng. Biomech. 14 (2012) 51–58.
[39] A. Kinaci, W. Bergmann, R.L.A.W. Bleys, A. van der Zwan, T.P.C. van Doormaal, Histologic comparison of the dura mater among species, Comp. Med. 70 (2020) 170–175. https://doi.org/10.30802/AALAS-CM-19-000022.
[40] A.Y. Sdobnov, M.E. Darvin, J. Schleusener, J. Lademann, V. V. Tuchin, Hydrogen bound water profiles in the skin influenced by optical clearing molecular agents—Quantitative analysis using confocal Raman microscopy, J. Biophotonics. (2019) 1–11. https://doi.org/10.1002/jbio.201800283.
[41] E. Guillard, A. Tfayli, M. Manfait, A. Baillet-Guffroy, Thermal dependence of Raman descriptors of ceramides. Part II: Effect of chains lengths and head group structures, Anal. Bioanal. Chem. 399 (2011) 1201–1213. https://doi.org/10.1007/s00216-010-4389-x.
[42] A. Jaafar, M.H. Mahmood, R. Holomb, L. Himics, T. Váczi, A.Y. Sdobnov, V. V. Tuchin, M. Veres, Ex-vivo confocal Raman microspectroscopy of porcine skin with 633/785-NM laser excitation and optical clearing with glycerol/water/DMSO solution, J. Innov. Opt. Health Sci. 2142003 (2021) 1–13. https://doi.org/10.1142/S1793545821420037.
[43] Spectragryph - optical spectroscopy software: Description, (n.d.). https://www.effemm2.de/spectragryph/about_descr.html (accessed October 17, 2020).
[44] D. Huang, W. Zhang, H. Zhong, H. Xiong, X. Guo, Z. Guo, Optical clearing of porcine

skin tissue in vitro studied by Raman microspectroscopy, J. Biomed. Opt. 17 (2012) 015004. https://doi.org/10.1117/1.jbo.17.1.015004.

[45] A.Y. Sdobnov, V. V. Tuchin, J. Lademann, M.E. Darvin, Confocal Raman microscopy supported by optical clearing treatment of the skin - Influence on collagen hydration, J. Phys. D. Appl. Phys. 50 (2017). https://doi.org/10.1088/1361-6463/aa77c9.

[46] P.J. Caspers, G.W. Lucassen, E.A. Carter, H.A. Bruining, G.J. Puppels, In vivo confocal raman microspectroscopy of the skin: Noninvasive determination of molecular concentration profiles, J. Invest. Dermatol. 116 (2001) 434–442. https://doi.org/10.1046/j.1523-1747.2001.01258.x.

[47] N. Nakagawa, M. Matsumoto, S. Sakai, In vivo measurement of the water content in the dermis by confocal Raman spectroscopy, Ski. Res. Technol. 16 (2010) 137–141. https://doi.org/10.1111/j.1600-0846.2009.00410.x.

[48] J.M. Hirshburg, K.M. Ravikumar, W. Hwang, A.T. Yeh, Molecular basis for optical clearing of collagenous tissues, J. Biomed. Opt. 15 (2010) 055002. https://doi.org/10.1117/1.3484748.

[49] P. Matousek, Raman signal enhancement in deep spectroscopy of turbid media, Appl. Spectrosc. 61 (2007) 845–854. https://doi.org/10.1366/000370207781540178.

[50] Y.A. Menyaev, D.A. Nedosekin, M. Sarimollaoglu, M.A. Juratli, E.I. Galanzha, V. V. Tuchin, V.P. Zharov, Optical clearing in photoacoustic flow cytometry, Biomed. Opt. Express. 4 (2013) 3030. https://doi.org/10.1364/boe.4.003030.

[51] B.H. Hokr, V. V. Yakovlev, Raman signal enhancement via elastic light scattering, Opt. Express. 21 (2013) 11757. https://doi.org/10.1364/oe.21.011757.

[52] Q. Zhang, K.L. Andrew Chan, G. Zhang, T. Gillece, L. Senak, D.J. Moore, R. Mendelsohn, C.R. Flach, Raman microspectroscopic and dynamic vapor sorption characterization of hydration in collagen and dermal tissue, Biopolymers. 95 (2011) 607–615. https://doi.org/10.1002/bip.21618.

[53] T.T. Nguyen, T. Happillon, J. Feru, S. Brassart-Passco, J.F. Angiboust, M. Manfait, O. Piot, Raman comparison of skin dermis of different ages: Focus on spectral markers of collagen hydration, J. Raman Spectrosc. 44 (2013) 1230–1237. https://doi.org/10.1002/jrs.4355.

[54] S.R. Utz, V.V. Tuchin, E.M. Galkina, The dynamics of some human skin biophysical parameters in the process of optical clearing after hyperosmotic solutions topical application, Vestn. Dermatol. Venerol. (2015) 60–68.

[55] V. Hovhannisyan, P.-S. Hu, S.-J. Chen, C.-S. Kim, C.-Y. Dong, Elucidation of the mechanisms of optical clearing in collagen tissue with multiphoton imaging, J. Biomed. Opt. 18 (2013) 046004. https://doi.org/10.1117/1.jbo.18.4.046004.

[56] J.J. Towey, A.K. Soper, L. Dougan, Molecular insight into the hydrogen bonding and micro-segregation of a cryoprotectant molecule, J. Phys. Chem. B. 116 (2012) 13898–13904. https://doi.org/10.1021/jp3093034.

[57] M.G. Tosato, R.S. Alves, E.A.P. Dos Santos, L. Raniero, P.F.C. Menezes, K.M.S. Belletti, C.E.O. Praes, A.A. Martin, Raman spectroscopic investigation of the effects of cosmetic formulations on the constituents and properties of human skin, Photomed. Laser Surg. 30 (2012) 85–91. https://doi.org/10.1089/pho.2011.3059.

[58] G. Pezzotti, M. Boffelli, D. Miyamori, T. Uemura, Y. Marunaka, W. Zhu, H. Ikegaya, Raman spectroscopy of human skin: looking for a quantitative algorithm to reliably estimate human age, J. Biomed. Opt. 20 (2015) 065008.

https://doi.org/10.1117/1.jbo.20.6.065008.

[59] S. Mujica Ascencio, C.S. Choe, M.C. Meinke, R.H. Müller, G. V. Maksimov, W. Wigger-Alberti, J. Lademann, M.E. Darvin, Confocal Raman microscopy and multivariate statistical analysis for determination of different penetration abilities of caffeine and propylene glycol applied simultaneously in a mixture on porcine skin ex vivo, Eur. J. Pharm. Biopharm. 104 (2016) 51–58. https://doi.org/10.1016/j.ejpb.2016.04.018.

[60] C. Choe, J. Lademann, M.E. Darvin, A depth-dependent profile of the lipid conformation and lateral packing order of the stratum corneum in vivo measured using Raman microscopy, Analyst. 141 (2016) 1981–1987. https://doi.org/10.1039/c5an02373d.

[61] C. Li, L.L. Chen, Y.Y. Wang, T.T. Wang, D. Di, H. Zhang, H.H. Zhao, X. Shen, J. Guo, Protein nanoparticle-related osmotic pressure modifies nonselective permeability of the blood– brain barrier by increasing membrane fluidity, Int. J. Nanomedicine. 16 (2021) 1663–1680. https://doi.org/10.2147/IJN.S291286.

[62] S. Cells, J.P. Wiebe, A. Kowalik, R.L. Gallardi, O. Egeler, B.H. Clubb, Glycerol Disrupts Tight Junction – Associated Actin, 21 (2000) 625–635.

[63] S. Gwer, H. Gatakaa, L. Mwai, R. Idro, C.R. Newton, The role for osmotic agents in children with acute encephalopathies: A systematic review, BMC Pediatr. 10 (2010). https://doi.org/10.1186/1471-2431-10-23.

[64] R. LaComb, O. Nadiarnykh, S. Carey, P.J. Campagnola, Quantitative second harmonic generation imaging and modeling of the optical clearing mechanism in striated muscle and tendon, J. Biomed. Opt. 13 (2008) 021109. https://doi.org/10.1117/1.2907207.

[65] C.M. Wu, H.H. Chen, K.H. Tseng, H.W. Chen, The effect of trifluoroethanol and glycerol on the thermal properties of collagen using optical displacement-enhanced heterodyne polarimeter, Appl. Sci. 5 (2015) 1184–1195. https://doi.org/10.3390/app5041184.

[66] Y. Alexandrovskaya, K. Sadovnikov, A. Sharov, A. Sherstneva, E. Evtushenko, A. Omelchenko, M. Obrezkova, V. Tuchin, V. Lunin, E. Sobol, Controlling the near-infrared transparency of costal cartilage by impregnation with clearing agents and magnetite nanoparticles, J. Biophotonics. 11 (2018). https://doi.org/10.1002/jbio.201700105.

[67] C. Calikoglu, M. Cakir, Y. Tuzun, Histopathological investigation of the effectiveness of collagen matrix in the repair of experimental spinal dura mater defects, Eurasian J. Med. 51 (2019) 133–137. https://doi.org/10.5152/eurasianjmed.2018.17422.

[68] W. Liu, X. Wang, J. Su, Q. Jiang, J. Wang, Y. Xu, Y. Zheng, Z. Zhong, H. Lin, In vivo Evaluation of Fibrous Collagen Dura Substitutes, Front. Bioeng. Biotechnol. 9 (2021) 1–12. https://doi.org/10.3389/fbioe.2021.628129.

[69] B. Khlebtsov, D. Bratashov, A. Burov, N. Khlebtsov, Tumor phantom with incorporated sers tags: Detectability in a turbid medium, Photonics. 8 (2021). https://doi.org/10.3390/photonics8050144.

[70] Z. Bao, B. Deng, Y. Zhang, X. Li, Z. Tan, Z. Gu, B. Gu, Z. Shao, W. Di, J. Ye, Ratiometric Raman nanotags enable intraoperative detection of metastatic sentinel lymph node, Biomaterials. 276 (2021) 121070. https://doi.org/10.1016/j.biomaterials.2021.121070.